

DEVELOPMENT OF NON-DESTRUCTIVE BEAM ENVELOPE MEASUREMENTS IN SRILAC WITH LOW BETA HEAVY ION BEAMS USING BPMs

T. Nishi*, T. Adachi, O. Kamigaito, N. Sakamoto, T. Watanabe, K. Yamada
RIKEN Nishina Center, Wako, Saitama, Japan

Abstract

The Superconducting RIKEN Linear accelerator (SRILAC) has been providing heavy ion beams of a few $p\mu\text{A}$ for the synthesis of new superheavy elements since June 2020, utilizing ten superconducting quarter-wavelength resonators. Although the beam supply has been stable, measurement and control of the beam dynamics in the SRILAC are critical to increasing the beam intensity up to $10 p\mu\text{A}$. However, destructive monitors cannot be used to avoid generating dust particles and outgassing. So far, the beam has been tuned by monitoring the beam center using Beam Energy Position Monitors (BEPMs) and vacuum monitors. In order to improve the beam control, we are developing a method for estimating the beam envelope by combining the quadrupole moments deduced from BEPMs, which consist of four cosine-shape electrodes, with calculations of the transfer matrix. While this method has been applied to electron and proton beams, it has not been practically demonstrated for heavy ion beams in beta ~ 0.1 regions. By combining BEPM simulations, we are making progress toward reproducing experimental results, overcoming specific issues associated with low beta beams. We will report on the current status of our developments.

INTRODUCTION: SRILAC AND PHASE ELLIPSE MEASUREMENT

SRILAC started the operation in 2020, and it has been providing a stable supply of heavy ion beam with intensity of a few $p\mu\text{A}$ and beam energy of about 6 MeV/u [1, 2]. In the future, the intensity is planned to increase up to $10 p\mu\text{A}$. SRILAC is also planned for medical isotope production and as an injector for the RI beam factory, where higher beam intensities are required. Precise measurement and control of the beam dynamics are essential to achieve stable operation in high-intensity conditions. However, there are no destructive monitors, such as wire scanners between SRF cavities to suppress dust production and outgassing. The only option to optimize the beam envelope inside the cavities is currently to minimize the vacuum levels between cavities. To estimate the beam dynamics in these sections, we perform Q scan measurement downstream, changing the magnetic field of quadrupole magnets several times and measure the beam profile for each magnetic field to reconstruct the phase ellipse. Based on the estimated phase ellipse downstream of SRF cavities, we can estimate the beam envelope with transfer matrices from the cavity sections to downstream

sections. The disadvantage of the Q-scan method is that we cannot perform the measurement frequently during beam supply to the users because it takes at least 30 minutes and we need temporary to change the magnetic fields. Another restriction of the method is to decrease the beam intensity to $\approx 100 \text{ enA}$ to avoid melting the wire and generating dust.

Therefore, we started to develop a new phase ellipse measurement method using non-destructive monitors, which can be applied to high-intensity beams and utilized for continuous measurements.

PRINCIPLE OF METHOD

In the new method, the beam envelopes are derived from the beam quadrupole moment $Q \equiv \sigma_x^2 - \sigma_y^2$ at several points in the beamline, which are measured by Beam Energy Profile Monitors (BEPMs), with the transfer matrices between the BEPMs [3]. Figure 1 shows the layout of SRILAC and beamline with 8 BEPMs in between SRF cavities. There are two types of BEPMs: type-A (numbers 1 to 6) with a longitudinal length of 50 mm and type-B (numbers 7 and 8) with a longitudinal length of 60 mm. These detectors were originally introduced to measure beam position and energy and have contributed significantly to the stable beam operation of SRILAC. The beam energy is calculated by measuring the time of flight from the time difference between signals in pairs of each section. Figure 2 shows the CAD model of type-A BEPMs on CST simulation. These BEPMs have cosine-like shape electrodes. This shape realizes the ideal response of the quadrupole moment while maintaining good linear position sensitivity [4]. The value of Q at each of the BEPMs is connected with the phase ellipses upstream using transfer matrices as

$$\begin{pmatrix} Q_1 \\ Q_2 \\ \vdots \\ Q_8 \end{pmatrix} = (\mathbf{H}, \mathbf{V}) \begin{pmatrix} \sigma_{xx}(0) \\ \sigma_{xx'}(0) \\ \sigma_{x'x'}(0) \\ \sigma_{yy}(0) \\ \sigma_{yy'}(0) \\ \sigma_{y'y'}(0) \end{pmatrix} \quad (1)$$

where

$$\mathbf{H} \equiv \begin{pmatrix} (M_{11}^{01})^2, 2M_{11}^{01}M_{12}^{01}, (M_{12}^{01})^2 \\ \vdots \\ (M_{11}^{08})^2, 2M_{11}^{08}M_{12}^{08}, (M_{12}^{08})^2 \end{pmatrix}, \quad (2)$$

$$\mathbf{V} \equiv \begin{pmatrix} -(M_{33}^{01})^2, -2M_{33}^{01}M_{34}^{01}, -(M_{34}^{01})^2 \\ \vdots \\ -(M_{33}^{08})^2, -2M_{33}^{08}M_{34}^{08}, -(M_{34}^{08})^2 \end{pmatrix}. \quad (3)$$

The quadrupole moment can be calculated based on the asymmetry of signal strength of four electrodes reflecting the flatness of

* takahiro.nishi@riken.jp

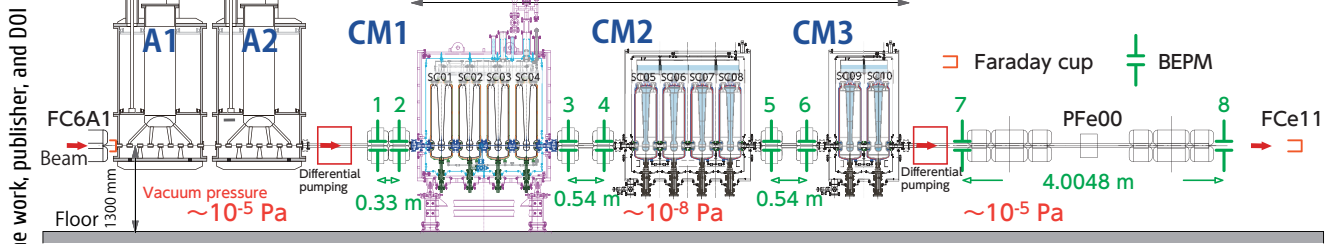


Figure 1: Schematic of beamline including SRILAC. Green numbers denote Beam Energy Position monitors, and PFe00 denotes a wire scanner.

a beam ellipse as

$$Q \equiv \sigma_x^2 - \sigma_y^2 = k_q \frac{V_L + V_R - V_U - V_D}{V_L + V_R + V_U + V_D} - \langle x \rangle^2 + \langle y \rangle^2, \quad (4)$$

where V_L , V_R , V_U , and V_D are the induced voltages of the left, right, up, and down electrodes, respectively, and k_q is a constant number measured previously.

In these equations, $\sigma(0)$ indicates the elements of the sigma matrix of the beam at the upstream position denoted as 0, and M_{ij}^{0n} is the (i, j) -th element of the transfer matrix from position 0 to the position of the n -th BEPM. The transfer matrices are calculated using the beam dynamics simulation software TraceWin. The simulation with TraceWin has been able to reproduce the beam energy response to changes in phase and voltage of each cavity at a level of 0.5% and also is expected to reproduce the realistic beam dynamics, including transfer matrices.

BIAS ON MEASUREMENT OF QUADRUPOLE MOMENT

Using this method, we first compared the Q variation during Q-scan measurements, as mentioned in Ref. [5]. While data showed clear positive correlations, there was also an offset between the measured values of the Q moments and those estimated with Q-scan. For investigation of the underlying cause, detailed simulations were conducted using CST Studio with the model shown in Fig. 2. Figure 3 shows the comparison of waveform signals from BEPM 7 (circles) and CST calculations (lines). For the simulations, the scaling factor and timing offset are tuned to reproduce the upstream

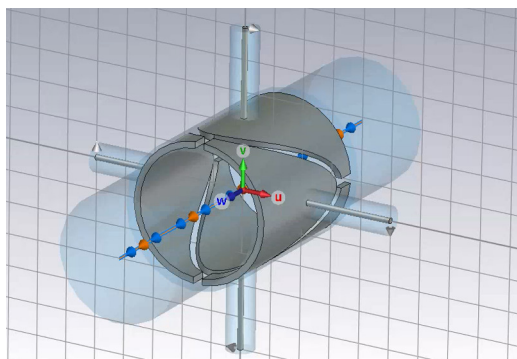


Figure 2: CAD model of type-A BEPM. The beam comes from the upper right corner towards the foreground. Up and down (right and left) electrodes are represented as upstream (downstream).

signals. In these simulations, the particle beam has no transverse emittances, i.e., $\sigma_x = \sigma_y = 0$. Despite the conditions, the peak of the signal from the downstream electrode is smaller than that from the upstream electrode. A similar tendency is shown in the measured data.

The result indicates this “bias” effect should be corrected in the quadrupole moment calculation based on eq. (4) to estimate phase ellipses accurately. This effect can be qualitatively understood as follows. When considering a cylindrical BEPM, if an electrode covers a portion of the circumference with an angle ϕ , the signal voltage V of that electrode is represented as a function of time t as

$$V(t) = \text{Re}[\sum_{n=0}^{\infty} V_n e^{jn\omega_0 t}], \quad (5)$$

$$V_n(\phi, L) = \frac{jn\omega_0 R}{1+jn\omega_0 RC} \frac{\phi L I_0}{\pi \beta c} \exp\left(\frac{n^2 \omega_0^2 \sigma_t^2}{2}\right). \quad (6)$$

R and C represent the resistance and the capacitance of the equivalent circuit of electrodes, and L is the longitudinal length of the electrodes. β , ω_0 , and σ_t denote velocity, angular velocity, and time widths of the beam, respectively. To account for the shape of the electrode, the electrode is divided longitudinally by δl and l -dependence of ϕ is incorporated as follows,

$$V(t) = \text{Re} \left[\int_0^L \sum_{n=0}^{\infty} V_n(\phi(l), \delta l) \exp\left(jn\omega_0 \left(t - \frac{l}{\beta c}\right)\right) dl \right]. \quad (7)$$

In the case of the upstream electrode, a large signal is generated corresponding to a large ϕ , followed by gradually overlapping

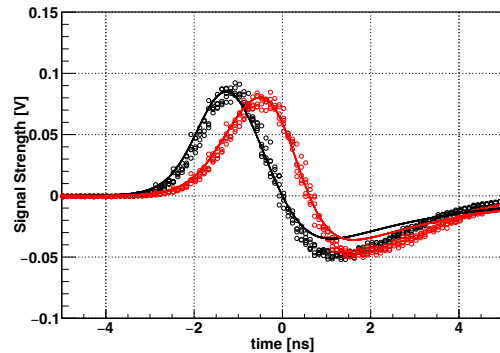


Figure 3: Waveform of the signals from BEPM electrodes. Black and red points correspond to upstream and downstream data, respectively. The lines represent the CST simulation result with the corresponding data color.

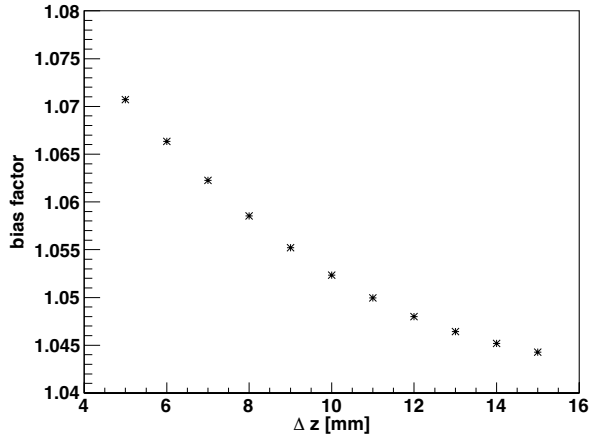


Figure 4: Longitudinal beam length ($\equiv \Delta z$) dependence of bias factor calculated by CST for type-A BEPM.

signals corresponding to smaller ϕ with a time delay. The peak maximum is mainly determined by the signal from the upstream portion of the electrode where ϕ is large. On the other hand, for the downstream electrode a relatively small signal is generated corresponding to small ϕ , followed by gradually overlapping signals corresponding to larger ϕ with a time delay. In the latter case, although the peak maximum is generated by the larger ϕ portion of the downstream electrode, the undershoot of the signal from the upstream portion overlaps, resulting in a relatively smaller peak than that of the upstream electrode. This effect is expected to have a greater impact when β and σ_t are smaller.

Incorporating this effect is necessary for an accurate determination of the phase ellipse. First, we calculated the dependency of this effect on the beam based on CST simulations. As commented above, this effect appears only for low *beta* particles. The deviation of the signal strength is tiny, 0.2%, for $\beta = 0.99$ [6, 7], but non-negligible, 5%, for $\beta = 0.1$. In the acceleration with our SRF cavities, particles are accelerated from $\beta = 0.09$ to 0.115, where the change of bias factor is small, at most 0.5%. For the longitudinal distribution of the beam, we vary spacial longitudinal widths Δz instead of σ_t in the CST calculation. Figure 4 shows the Δz dependence of the bias effect. Here, bias is defined as the ratio of signal strength between that from the upstream and that from the downstream. As shown, there is relatively large dependence on Δz . Although the longitudinal distribution of the beam has not been measured directly, considering that the RF of SRILAC is 73 MHz, it is reasonable to assume that it falls within the range of 5 to 15 degrees (1 rms), which corresponds to approximately 5 mm to 15 mm in terms of the longitudinal distribution. The bias factor changes by approximately 3% in this range. Therefore, in the subsequent analysis we consider these values as an uncertainty of the bias factor and treat them as errors of Q , which typically corresponds to 4 to 5 mm^2 shift.

APPLICATION FOR PHASE ELLIPSE MEASUREMENT

For the application of this method, we estimated the bias factor by comparing it with the Q-scan measurement result because the CST simulation does not fully reproduce the measured waveform

Table 1: Estimated Parameters of Phase Ellipse

Method	bias	ϵ_h	ϵ_v	α_h	β_h	α_v	β_v
BEPM	not corrected	3.2	0	-4.9	0.9	-	-
BEPM	corrected	6.7	2.6	-0.5	0.3	1.1	1.7
BEPM + PF	corrected	5.9	4.0	-0.6	0.2	0.7	0.6
Q-scan	-	5.3	3.8	0.5	0.3	0.6	0.4

signals, as shown in Fig. 2. For the bias factor estimation, the measured data in April 2023 are utilized. As a result, the bias factors were determined to reproduce those results to be 1.060 for type-A BEPMs and 1.044 for type-B BEPMs.

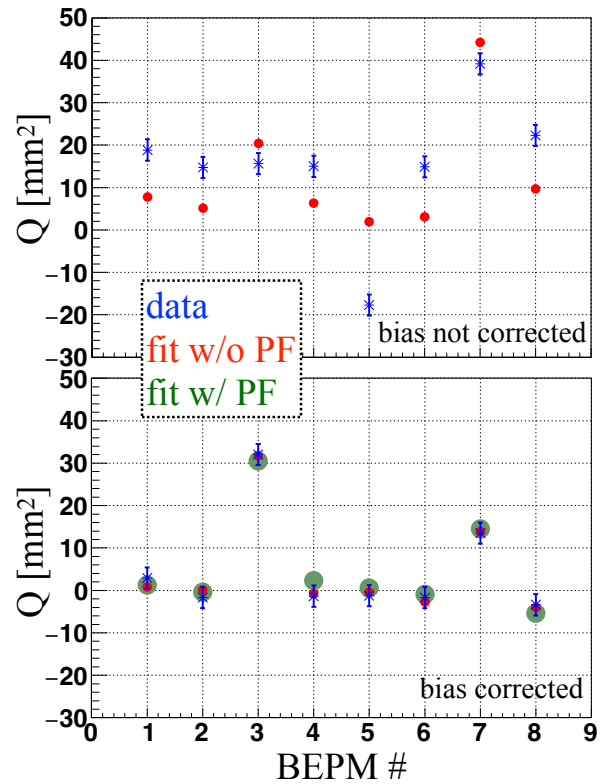


Figure 5: Measured and fitted quadrupole moment Q at each BEPM position. The top (bottom) graph corresponds to the calculation without (with) bias factor correction. The green circle is a fit result of the analysis using additional profilometer data.

To demonstrate the method, we again compared the estimated phase ellipses with these by Q-scan method using data in 2-month later, on June 16th, 2023. In this period ion source was restarted several times, and some accelerator parameters, such as slit, were tuned. Therefore it is a good demonstration if the method can reproduce the result by the conventional Q-scan method. Figure 5 shows the measured quadrupole moments Q s for 8 BEPMs before and after bias correction. In the analysis, we estimate phase ellipse upstream to reproduce the measured Q of each BEPM. The calculated Q s with the estimated phase ellipse are also shown in the graphs. The analysis with the wire scanner at e00 in Fig. 1, which

is represented as a profil monitor or PFe00, is also performed. The additional information of the PF is expected to increase the sensitivity of the analysis to the absolute values of beam emittances.

As shown in the Fig. 5, the Q s without bias correction were not reproduced. In contrast, the Q s are well reproduced in both analyses without and with profil monitor data after the bias correction. The calculated Q s with these two methods show a tiny difference. However, the estimated phase ellipse parameters, summarized in Table 1, show large differences between these analyses. For the analysis with only BEPMs after bias correction, ϵ_h and ϵ_v differ significantly, indicating that realistic solutions have not been achieved. This result may be attributed to the limited number of BEPMs in our case compared to previous studies, resulting in relatively low sensitivity to absolute values of σ_x and σ_y . By contrast, the values of ϵ_h and ϵ_v become closer and more realistic by the analysis including the PF data.

The results of the obtained phase ellipses with BEPMs and PF data are compared with the results of the Q-scan method, as shown in Fig. 6 and Table 1. The estimated values of ϵ_h and ϵ_v closely match with an accuracy of approximately 10%. Furthermore, the phase ellipse parameters also exhibit very similar values. While the correlation for the horizontal ellipse are reversed, it corresponds to approximately only 15 cm shift of the focused point. In conclusion, these results show sufficiently good agreements as a first step of the development.

It should be noted that adding PF data when applying this method does not produce significant problems. The measurements with profil monitors are performed regularly once a day to verify the beam stability during normal operation. By utilizing these data, it is possible to operate without additional destructive measurements. Moreover, compared to Q-scan measurements, which require changing the magnetic field this method requires only one profil monitor measurement without magnetic field adjustments.

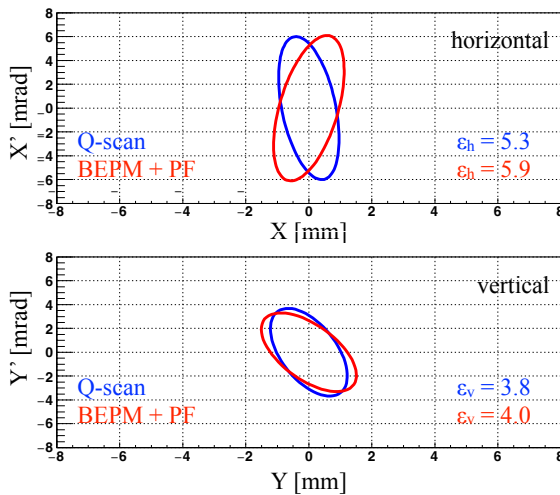


Figure 6: Estimated phase ellipses by the conventional Q-scan method and this work.

CONCLUSION AND FUTURE PERSPECTIVES

To estimate the beam dynamics in superconducting RF cavities, we developed a new approach leveraging BEPM signals. Although

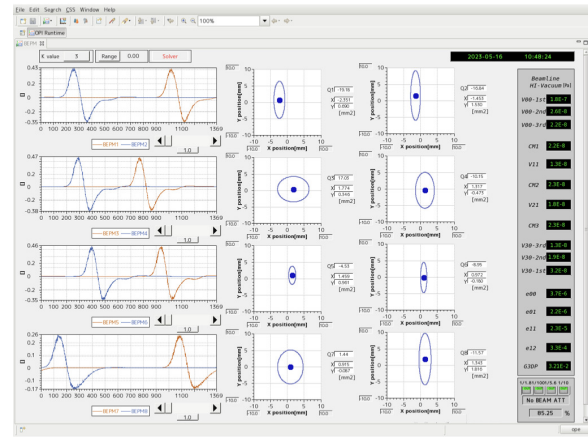


Figure 7: Operation monitor for BEPMs. On the left side averaged waveform of each BEPM is shown. On the right side, the estimated beam position and spatial distribution are displayed.

this method has been recognized for several decades, we found bias factors arising with low-beta particles and co-sin like shapes of BPM are important to estimate the real Q moments of the beams. By conducting compensated analysis, we have successfully reproduced the phase ellipse observed through the Q-scan method. Visualizations of the estimated phase ellipses have already been integrated into our daily monitoring systems as shown in Fig. 7. To further validate the accuracy of this method, we plan to gather additional data and integrate it into our routine operations to achieve more precise beam tuning. Going forward, we aim to implement this methodology across the entire RI Beam Factory.

ACKNOWLEDGMENTS

We thank Prof. Toyama for the discussion about the new method with BPMs, and our colleague Dr. Fukunishi for the discussion in the early stage of the development. We are also grateful to all operation staff for SRILAC, who help us perform all kind of measurements for the development.

REFERENCES

- [1] K. Yamada *et al.*, “Successful Beam Commissioning of Heavy-Ion Superconducting Linac at RIKEN”, in *Proc. SRF’21*, East Lansing, MI, USA, Jun.–Jul. 2021, paper MO0FAV01, pp.167–174, 2021. doi:10.18429/JACoW-SRF2021-MO0FAV01
- [2] H. Sakai, H. Haba, K. Morimoto, and N. Sakamoto, “Facility upgrade for superheavy-element research at RIKEN”, *Eur. Phys. J. A*, vol. 58, pp. 1–15, 2022. doi:10.1140/epja/s10050-022-00888-3
- [3] R. H. Miller, J. E. Clendenin, M. B. James, and J. C. Sheppard, “Nonintercepting Emittance Monitor”, in *Proc. HEAC’83*, Fermilab, IL, USA, pp. 603-605, 1983.
- [4] T. Watanabe *et al.*, “Commissioning of the Beam Energy Position Monitor System for the Superconducting RIKEN Heavy-ion Linac”, in *Proc. IBIC’20*, Santos, Brazil, Sep. 2020, paper FRA004, pp. 295–302, 2020. doi:10.18429/JACoW-IBIC2020-FRA004
- [5] T. Nishi *et al.*, “Beam Acceleration with the Upgraded RIKEN Heavy-Ion LINAC”, in *Proc. HB’21*, Batavia, IL, USA, Oct. 2021, paper THBC1, pp. 231–234, 2021. doi:10.18429/JACoW-HB2021-THBC1

- [6] T. Suwada, K. Furukawa, and M. Satoh, "Development of a New Beam-Energy-Spread Monitor Using Multi-Stripline Electrodes", in *Proc. PAC'03*, Portland, OR, USA, May 2003, paper ROAB012, pp. 533-535, 2003.
doi:10.1109/PAC.2003.1288969
- [7] M. Tajima, T. Koseki, T. Nakaya, and T. Toyama, "Development of 16 Electrodes Beam-size Monitors for J-PARC MR", in *Proc. IBIC'19*, Malmö, Sweden, Sep. 2019, paper TUPP021, pp. 347-350, 2019.
doi:10.18429/JACoW-IBIC2019-TUPP021